Journal of Inorganic Biochemistry 192 (2019) 45–51

Contents lists available at ScienceDirect

Journal of Inorganic Biochemistry

journal homepage: www.elsevier.com/locate/jinorgbio

Interaction of Cm(III) with human serum albumin studied by time-resolved laser fluorescence spectroscopy and NMR

Nicole Adam[a,*], Christian Adam[a], Markus Keskitalo[a,c], Jonathan Pfeuffer-Rooschüz[b], Petra J. Panak[a,b]

[a] Karlsruhe Institute of Technology (KIT), Institute for Nuclear Waste Disposal (INE), P.O. Box 3640, 76021 Karlsruhe, Germany
[b] University of Heidelberg, Institute of Physical Chemistry, Im Neuenheimer Feld 253, 69120 Heidelberg, Germany
[c] Department of Chemistry - Radiochemistry, University of Helsinki, P.O. Box 55, 00014 Helsinki, Finland

ARTICLE INFO

Keywords:
Human serum albumin
Actinides
Cm(III)
Spectroscopy
Complexation

ABSTRACT

The complexation of Cm(III) with human serum albumin (HSA) was investigated using time-resolved laser fluorescence spectroscopy (TRLFS). The Cm(III) HSA species is dominating the speciation between pH 7.0 and 9.3. The first coordination sphere is composed by three to four H_2O molecules and five to six coordinating ligands from the protein. For the complex formation at pH 8.0 a conditional stability constant of $\log K = 6.16 \pm 0.50$ was determined. Furthermore, information on the Cm(III) HSA binding site were obtained. With increasing Cu(II) concentration the Cm(III) HSA complexation is suppressed whereas the addition of Zn(II) has no effect. This points to the complexation of Cm(III) at the N-terminal binding site (NTS) which is the primary Cu(II) binding site. NMR experiments with Cu(II), Eu(III) and Am(III) HSA show a decrease of the peak assigned to the His C2 proton of His 3, which is part of the NTS, with increasing metal ion concentration. This confirms the complexation of Eu(III) and Am(III) at the Cu(II) binding site NTS. The results presented in this study contribute to a better understanding of relevant biochemical reactions of incorporated actinides.

1. Introduction

Accidentally released radionuclides, in particular actinides, can cause a serious health risk upon incorporation. Apart from the chemical toxicity, their hazardousness depends mainly on the high radiological toxicity [1]. Actinides have no essential function in the biochemistry of the human body and up to now little is known about the mechanisms of uptake, transport and storage in man. Regarding the development of potential decontamination therapies, a detailed understanding of the relevant biochemical reactions of incorporated actinides is strongly required [2].

Incorporated actinides preferentially interact with blood serum components before accumulating in the organs (bone, liver, kidneys etc.) [3,4]. One representative of utmost importance is human serum albumin (HSA), the most abundant protein in the human blood plasma (~60% of total protein, 3.5–5 g/dL) [5]. HSA is a single-chain protein with a molecular mass of 66.5 kDa. It consists of three homologous domains, each comprised of two subdomains with mainly α-helices connected by flexible loops [6,7]. Besides its contribution to the regulation of the colloid osmotic pressure, HSA binds and transports a range of predominantly water-insoluble molecules such as fatty acids, hormones, bilirubin, heme, drugs as well as metal ions (such as Na^+, Ca^{2+}, Cu^{2+} and Zn^{2+}). Although there is still a lack of detailed structural information, it is known that most mammalian albumins including HSA have at least four metal ion binding sites: the amino terminal Cu and Ni binding site (ATCUN site, also known as N-terminal site, NTS), the Multi-Metal Binding Site (MBS, also known as Site A), the site around Cys-34 and Site B, which location is still unknown [6–11]. The NTS or ATCUN site is composed of the first three amino acids Asp-Ala-His of the albumin sequence [6,7]. Probably the fourth residue, Lys, is also involved in metal ion binding [12]. An important characteristic of the NTS is the involvement of nitrogen of the peptide bonds in the coordination of metal ions. Together with the N-terminal NH_2 group and His-3 a square-planar complexation environment for metal ions like Cu(II) and Ni(II) is formed [13]. At Site A two His residues (His-67 and His-247), Asn-99 and Asp-249 are involved in metal ion binding [8,14]. Since many different metal ions bind to Site A, it is also known as “multi-metal binding site”, MBS. It is the preferential site for Zn(II) and one of two favoured sites for Cd(II) binding [15–17]. Furthermore, the MBS can also bind Cu(II) and Ni(II) to a certain extent [16,18]. The site around Cys-34 and site B which is the second Cd(II) site are less well characterized. The preferences of several transition

* Corresponding author.
E-mail address: nicole.adam@kit.edu (N. Adam).

https://doi.org/10.1016/j.jinorgbio.2018.12.007
Received 9 October 2018; Received in revised form 16 November 2018; Accepted 15 December 2018
Available online 20 December 2018
0162-0134/

metal ions for the different HSA binding sites are described in the literature [18–26]. However, a quantitative comparison of the data is difficult since the interaction mechanisms are complicated and different methods and conditions were applied for the determination of the stability constants. Nevertheless, a list of relative affinities of Cu(II), Ni (II), Zn(II), Co(II), Cd(II) and V(IV)O to the HSA binding sites NTS, MBS and Site B has been derived: [19].

NTS: Cu(II) ≫ VO(IV) ≫ Ni(II) ≫ Co(II)

MBS: VO(IV) > Cu(II) ≫ Zn(II) > Cd(II) > Ni(II) > Co(II)

Site B*: Cd(II) > Co(II)

* High uncertainty of the binding affinity of Zn(II) at this site.

It is well-known that HSA forms complexes with a wide range of metal ions, especially transition metals. However, up to now only very few data regarding the interaction of lanthanides and actinides with albumin is reported [27–34]. Most of them are phenomenological studies using methods like UV/Vis spectroscopy, FT-IR spectroscopy, fluorescence spectroscopy and equilibrium dialysis. They give only semiquantitative results and provide no information on the complexation mechanism, binding structure and number of species. Schomäcker et al. derived conditional stability constants for HSA complexes of the lanthanides Ce, Nd, Eu, Dy, Ho, Er and Tm at pH 7.4, T = 310 K and physiological ionic strength (150 mM) using equilibrium dialysis [30]. The logK values increase with decreasing ionic radius of the Ln(III) ions from 4.90 (Ce(III)) to 8.90 (Tm(III)). Regarding the actinides, only the interaction of Th(IV) and U(VI) with HSA has been investigated so far. Michon et al. identified two binding sites for U(VI) using fluorescence quenching methods [33]. The stronger site seems to be the NTS, for which a stability constant of logK = 10.8 (pH 7.4) was determined by Montavon et al. [32] Ali et al. showed that U(VI) and Th(IV) (as well as Ce(IV)) interact with carbonyl and amide groups of HSA, with U(VI) showing a slightly higher binding affinity than Th(IV) [31]. Furthermore, Ce(IV), Th(IV) and U(VI) seem to alter the secondary conformation of HSA. Circular dichroism measurements show a decrease of the α-helix content indicating a partial unfolding of the protein.

Most studies on HSA interaction with lanthanides and actinides give only a qualitative description of the complexation reaction but do not provide information on the binding site(s) and the detailed structure of the complexes. Data on the binding of trivalent actinides with HSA is not available. In the present study Cm(III) is used as a representative of the trivalent actinides because of its excellent fluorescence properties [35]. The interaction of HSA with Cm(III) is studied using time-resolved laser fluorescence spectroscopy (TRLFS). This is a very sensitive method for determination of the speciation of lanthanides and actinides in submicromolar concentration ranges [36]. Shape and position of the emission bands as well as the fluorescence lifetime provide information on the coordination environment of the metal ion. The present work focuses on the interaction of Cm(III) with HSA as a function of pH, temperature and protein concentration to identify and characterize the Cm(III) HSA species. Furthermore, competition titrations with Cu(II) and Zn(II) provide information on the preferential HSA binding site of Cm(III). These results are confirmed by NMR (nuclear magnetic resonance) experiments with Cu(II), Eu(III) and Am(III) albumin, yielding further insight into the structures of the different complexes.

2. Experimental

2.1. Chemicals and sample preparation

The protein samples were prepared in TRIS (2-Amino-2-(hydroxymethyl)propane-1,3-diol) or HEPES (2-[4-(2-hydroxyethyl)piperazin-1-yl]ethanesulfonic acid) buffered solutions (10 mM, pH 7.4) with a physiological sodium chloride concentration of 150 mM NaCl using ultrapure water (Millipore, Billerica, MA, USA; 18.2 MΩ cm). Human serum albumin of high reagent grade (lyophilized powder, fatty acid free, globulin free, ≥99%) was purchased from Sigma-Aldrich and purified before use by size exclusion chromatography (Sephadex G-25 medium, GE Healthcare) and filtration (Amicon Ultra-4 Centrifugal Filter Units, 30 kDa) according to the protocol of Harris et al. [37,38]. The protein concentration of the HSA stock solution was determined by UV/Vis spectroscopy at λ = 280 nm using an extinction coefficient of ε = 35 296 $M^{-1}{\cdot}cm^{-1}$ [39].

The Cm(III) stock solution used for the TRLFS studies (c(Cm) = $2.12{\cdot}10^{-5}$ M in H_2O) had an isotopic mass distribution of 89.7% ^{248}Cm, 9.4% ^{246}Cm, and ≤ 1% ^{243}Cm, ^{244}Cm, ^{245}Cm and ^{247}Cm. The Cm(III) concentration of the TRLFS samples was adjusted to $1.00{\cdot}10^{-7}$ M by adding 4.7 µl of the Cm(III) stock solution to 970 µl of the buffered HSA solution with a concentration of $4.85{\cdot}10^{-6}$ M, resulting in a final HSA concentration of $5.00{\cdot}10^{-6}$ M.

Complexation studies were carried out at varying pH values between 3.5 and 11.0. The pH was adjusted stepwise starting from pH 7.4 downwards to pH 3.5 and upwards to pH 11.0 using HCl and NaOH solutions of different concentrations (1.0 M, 0.1 M, and 0.01 M). For the titration experiment, the Cm(III) concentration (c(Cm (III)) = $1.00{\cdot}10^{-7}$ M) and the pH were kept constant. The HSA concentration ranged from 0 to $8.26{\cdot}10^{-6}$ M. For the competition titration experiments, the Cm(III) and HSA concentrations were fixed at c(Cm (III)) = $1.00{\cdot}10^{-7}$ M and c(HSA) = $5.00{\cdot}10^{-6}$ M at pH 8.0. $ZnCl_2$ or $CuCl_2$ solution (10^{-2} M) was added stepwise up to a total concentration of c(Cu(II)) = $5.00{\cdot}10^{-5}$ M and c(Zn(II)) = $1.20{\cdot}10^{-4}$ M. TRLFS measurements were performed at room temperature (296 K) and physiological temperature (310*K*). The pH electrode was calibrated at each temperature.

For the NMR experiments, samples with a total volume of 1 ml containing 1 mM HSA and 10 mM TRIS in a 9:1 H_2O/D_2O mixture were prepared. Deuterium oxide was purchased from Euriso-Top GmbH. The pH was adjusted to 8.0 and aliquots of a Cu(II), Eu(III) or Am(III) stock solution were added stepwise until a metal ion concentration of 2 mM was reached. The Cu(II) and Eu(III) stock solutions were prepared from $CuCl_2$ and $EuCl_3$, respectively (0.1 M). For the titration with Am(III), an aliquot of the Am(III) stock solution, containing 493 µg $^{243}Am(NO_3)_3$ and traces of $^{241}Am(NO_3)_3$ in 0.4 mL 0.5 mol·L^{-1} HNO_3 was heated until dry to reduce the nitrate content. The remaining $Am(NO_3)_3$ was dissolved in 100 µL 0.5 mol·L^{-1} hydrochloric acid to obtain a solution containing 20 mol·L^{-1} Am(III). After each titration step, the pH was controlled and a NMR spectrum was recorded. All preparations of radioactive samples were performed in a dedicated fume hood. Gastight J. Young type NMR tubes were used for radioactive samples.

2.2. Time-resolved laser fluorescence spectroscopy

TRLFS was performed using a Nd-YAG (Yttrium Aluminium Garnate, Continuum Surelite Laser) pumped dye laser system (NARROWscan D-R Dye Laser) with a repetition rate of 10 Hz. Cm(III) was excited using a wavelength of 396.6 nm. Emission spectra were recorded in the range of 575 to 635 nm after a delay time of 1 µs to discriminate short-lived fluorescence of organic compounds. After spectral decomposition by a spectrograph (Shamrock 303i) with a 1199 lines/mm grating, the spectra were recorded with an ICCD (intensified charge-coupled device) camera (iStar Gen III, ANDOR) containing an integrated delay controller. For better comparison, all spectra were normalized to the same peak area. For lifetime measurements, the delay time between the laser pulse and the detection of the fluorescence emission was increased continuously with time intervals of Δt = 20 µs. The lifetime τ is obtained by fitting the fluorescence intensity I as a function of the delay time t according to

$$I(\lambda) = I_0(\lambda) \bullet e^{-t/\tau} \quad (1)$$

with the initial intensity I_0 at t = 0. The number of water molecules in

the first coordination sphere is obtained from the fluorescence lifetime τ (in ms) using the Kimura equation [40,41].

$$n_{H_2O} = 0.65 \cdot \frac{1}{\tau} - 0.88. \quad (2)$$

2.3. NMR spectroscopy

All NMR spectra were recorded at $T = 298$ K on a Bruker Avance III 400 spectrometer operating at a resonance frequency of 400.18 MHz for ^{1}H nuclei. The spectrometer was equipped with a z-gradient inverse room temperature probe optimized for ^{1}H detection. Chemical shifts are referenced internally to TMS (Tetramethylsilane, δ(TMS) = 0 ppm) by the deuterium lock signal of D_2O. For single scan ^{1}H spectra, standard 90° pulse sequences were used. Water suppression was achieved by the WATERGATE pulse sequence [42,43]. All spectra were recorded with 32 k data points and are zero filled to 64 k points. For WATERGATE spectra, 64 scans were acquired per spectrum with a relaxation delay of 2 s. Exponential window functions with a line broadening factor of 0.05 Hz were applied for processing.

3. Results and discussion

3.1. Complexation studies of Cm(III) with HSA at varying pH

The normalized fluorescence spectra of Cm(III) with HSA in the pH range from 3.5 to 11.0 at room temperature (296 K) are shown in Fig. 1. The spectra reveal a strong pH dependency of the complexation reaction. Up to pH 6.7 the spectrum is dominated by the fluorescence of the Cm(III) aquo ion, displaying an emission band at $\lambda_{max} = 593.8$ nm [44–46]. With increasing pH the emission band shifts to higher wavelengths. Simultaneously, the emission band broadens, which indicates the presence of at least two different Cm(III) species. Comparison with Cm(III) spectra measured in the absence of HSA (data not shown) shows that the main contribution to the emission band results from Cm(III) interaction with the solvent TRIS-H_2O-OH^- ($\lambda_{max} = 598.3$ nm). Furthermore, at pH ≥ 6.0 a Cm(III) HSA species is formed ($\lambda_{max} = 602.6$ nm). The ratio of this species increases with increasing pH. Due to the increasing OH^- concentration, a continuous shift of the emission band up to 603.0 nm at pH 9.3 is observed. Above pH 9.7 the intensity decreases significantly and the emission band broadens due to the hydrolysis of Cm(III). However, a significantly higher drop of intensity would be expected if only Cm(III) hydrolysis species are present,

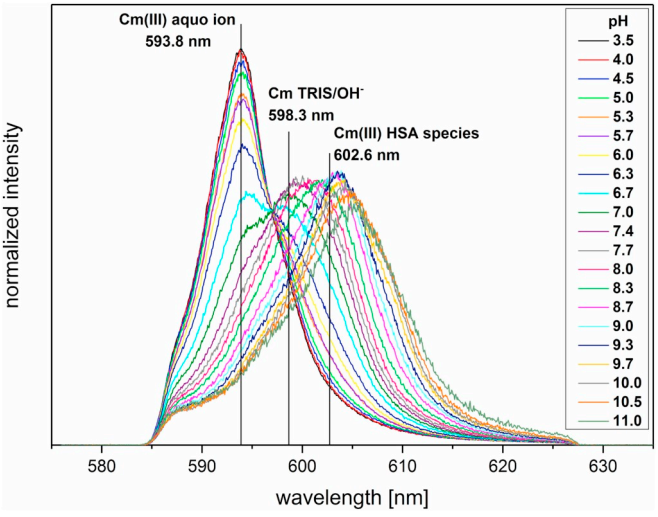

Fig. 1. Normalized fluorescence spectra of Cm(III) with HSA in the pH range between 3.5 and 11.0; c(Cm) = $1.0 \cdot 10^{-7}$ M, c(HSA) = $5.0 \cdot 10^{-6}$ M, TRIS 10 mM, NaCl 150 mM, $T = 296$ K.

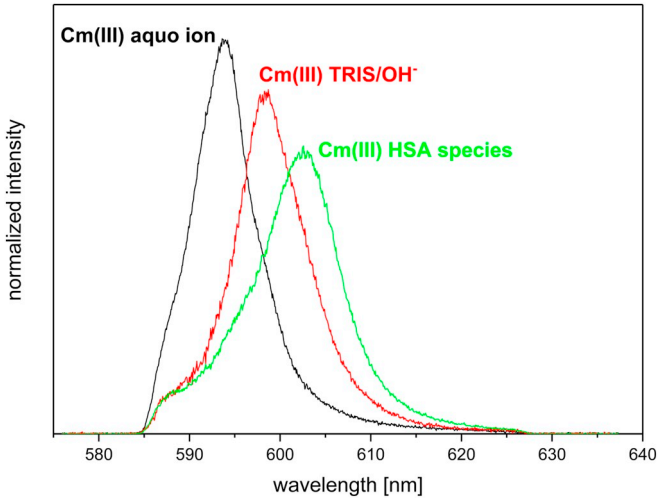

Fig. 2. Normalized fluorescence spectra of the Cm(III) aquo ion, the Cm(III) TRIS/OH^- solvents species and the Cm(III) HSA species.

indicating the existence of ternary Cm(III)-OH-HSA species. This shows that the complexation of Cm(III) with HSA plays a significant role in the alkaline pH region as well.

The shift of the emission band of a Cm(III) complex species relative to the emission band of the Cm(III) aquo ion results from an increased ligand field splitting of the complex species and is related to the complexation strength of the ligands. The emission band of the Cm(III) HSA species is shifted about 10 nm relative to the aquo ion. As shown in a recent study for Cm(III) transferrin ($\lambda_{max} = 619.9$ nm) the internalization of Cm(III) into the protein structure upon complexation at the transferrin binding sites results in a significantly higher bathochromic shift [47]. Therefore, an internalization of Cm(III) into the HSA protein structure can be excluded. Instead, the Cm(III) HSA complexation is characterized by inner-sphere complex formation resulting from the interaction of Cm(III) with amino acid residues of the protein.

The fluorescence spectra of the three components were determined from the pH dependent fluorescence spectra (Fig. 2). These represent the Cm(III) aquo ion, the Cm(III) TRIS/OH^- solvent species and the Cm (III) HSA species. The fractions of these species at various pH values were determined by peak deconvolution (species distribution, Fig. 3). Since the total fluorescence intensity is constant during the experiments, the fluorescence intensity factors ($f_i = I_{complex}/I_{aquo\ ion}$) of the

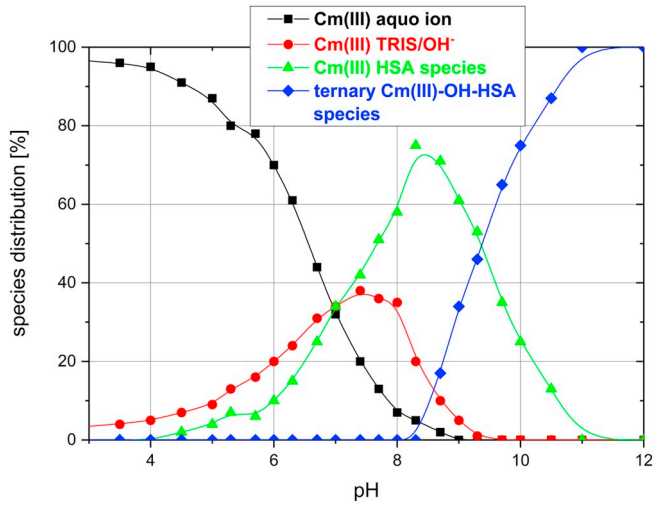

Fig. 3. Speciation of Cm(III) with HSA as a function of pH; c (Cm) = $1.0 \cdot 10^{-7}$ M, c(HSA) = $5.0 \cdot 10^{-6}$ M, TRIS 10 mM, NaCl 150 mM, $T = 296$ K.

different species are assumed to be 1. Therefore, the fractions of the peak areas equal the species concentrations. The Cm(III) aquo ion dominates the speciation up to pH 6.8. The Cm(III) TRIS/OH^- solvent species is present over a wide pH range up to pH 8.3 and reaches a maximum ratio of about 40% at the physiological pH 7.4. The Cm(III) HSA species is formed in the pH range from 4.0 to 11.0 and becomes the dominating species between pH 7.4 and 8.7. At pH ≥ 8.3 ternary Cm (III)-OH-HSA species are formed and dominate the speciation at pH ≥ 9.3.

In order to characterize the Cm(III) HSA species, the fluorescence lifetime was determined. As the species does not exist as a pure component at any pH value between 6.0 and 9.0 the decay of the fluorescence emission of Cm(III) as a function of the delay time was fitted using a bi- or triexponential decay function (depending on the pH) considering the fluorescence lifetimes of the Cm(III) aquo ion (τ = 65 µs), the $Cm(OH)^{2+}$ (τ = 72 µs) and $Cm(OH)_2^{+}$ (τ = 80 µs) species [48,49]. This procedure yields an average fluorescence lifetime of τ = 152 ± 10 µs for the Cm(III) HSA species. Assuming an overall coordination number of nine for Cm(III), the fluorescence lifetime corresponds to three to four H_2O molecules and five to six coordinating ligands in the first coordination sphere of Cm(III) [40,41]. These are mainly amino acids from the protein and potentially additional anions like OH^-, CO_3^{2-} etc. The fluorescence lifetime of the Cm(III) HSA species is significantly shorter compared to that of the Cm(III) transferrin species with complexation of Cm(III) at the C-terminal binding site of transferrin (τ = 220 µs) [47]. Complexation of Cm(III) at the transferrin binding site leads to an "internalization" of Cm(III) into the protein structure. The majority of the water molecules in the first coordination sphere are replaced by coordinating ligands from the protein and carbonate ions as synergistic anions resulting in a significantly longer fluorescence lifetime. In case of the Cm(III) HSA species there are still three to four water molecules present in the first coordination sphere confirming the formation of a comparably weaker inner sphere complex with the protein. This is in good agreement with the spectroscopic shift of the emission band of the Cm(III) HSA species and hints to binding of Cm(III) at the NTS, since the N-terminal end of the protein chain is very flexible and easily accessible.

3.2. Complexation studies of Cm(III) with HSA at varying HSA concentrations

The complexation of Cm(III) with HSA was studied in dependence of the HSA concentration (c(HSA) = 0–8.26·10^{-6} M) at a fixed pH of 8.0 (Fig. 4). The spectrum obtained in the absence of HSA represents the Cm(III) solvent spectrum at pH 8.0 with an emission maximum at λ_{max} = 598.7 nm. With increasing HSA concentration the ratio of the Cm(III) HSA species increases, resulting in a continuous shift of the emission band up to λmax = 601.6 nm.

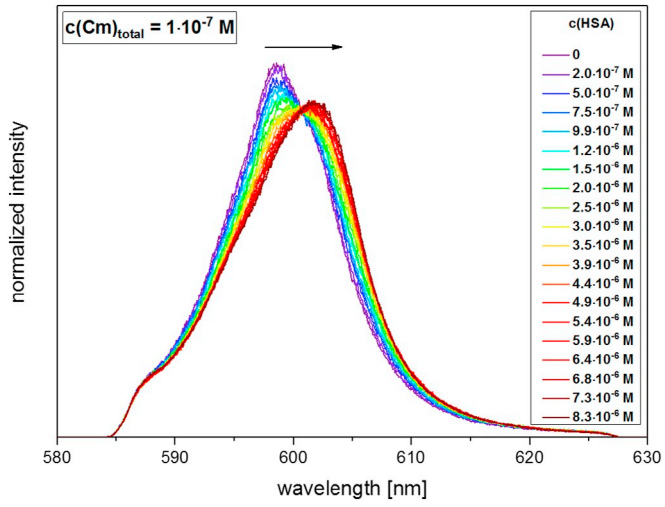

Fig. 4. Normalized fluorescence spectra of Cm(III) with increasing HSA concentration at pH 8.0; c(Cm) = 1.0·10^{-7} M, c(HSA) = 0–8.26·10^{-6} M, TRIS 10 mM, NaCl 150 mM, T = 296 K.

The complexation of Cm(III) with HSA is described by the following equations:

$$Cm(III) + HSA \rightleftharpoons CmHSA \quad (3)$$

$$K = \frac{[CmHSA]_{eq}}{[Cm]_{eq}\,[HSA]_{eq}} \quad (4)$$

$$\log \frac{[CmHSA]_{eq}}{[Cm]_{eq}} = \log[HSA]_{eq} + \log K \quad (5)$$

The equilibrium constant of the Cm(III) HSA species is defined according to Eq. 4. Transformation to Eq. 5 gives a linear correlation of the logarithm of the concentration ratio [CmHSA]/[Cm(III)] and the logarithm of the free HSA concentration. The slope represents the number of coordinating ligands in the Cm(III) complex (slope analysis). For the slope analysis the equilibrium concentrations of Cm(III), HSA and the Cm(III) HSA species are required. They are calculated using the species distribution in dependence of the HSA concentration obtained by peak deconvolution and Eqs. (6) and (7).

$$[Cm(III)]_{eq} = [Cm(H_2O)_9{}^{3+}] \quad (6)$$

$$[HSA]_{eq} = [HSA]_{tot} - [CmHSA] \quad (7)$$

Fig. 5 shows the slope analysis of the Cm(III) HSA complexation. The linear regression of the double logarithmic plot has a slope of 1.06 indicating the formation of a 1:1 Cm(III) HSA complex. Due to steric reasons, the coordination of a second protein molecule can be ruled out. This is comparable to the results obtained for Cm(III) transferrin which also forms a complex with 1:1 stoichiometry under similar experimental conditions [50].

Using Eq. (4), the conditional stability constant of the Cm(III) HSA species is calculated to be logK = 6.16 ± 0.50. Since the coordinating amino acid residues in the Cm(III) HSA complex are not yet explicitly determined, their pK_a values cannot be considered for the calculation of a pH independent logK value. The relatively large error of the stability constant is due to the fact that the measurements are performed at pH 8.0 with the ratio of the Cm(III) aquo ion, which represents $[Cm]_{eq}$, being ≤10% for each titration step. Even small changes of ± 1% of the $[Cm(H_2O)_9]^{3+}$ fraction and therefore $[Cm]_{eq}$ have a significant impact on the logarithmic stability constant.

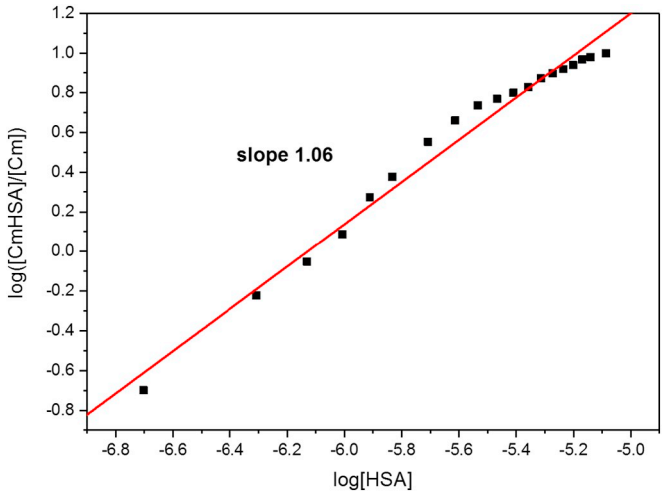

Fig. 5. Double logarithmic plot of the concentration ratio [CmHSA]/[Cm] vs. [HSA].

Since Cm(III) and Eu(III) have similar effective ionic radii ($IR_{Eu(III)}$ = 0.950 Å, $IR_{Cm(III)}$ = 0.98 Å) [51] and comparable chemical properties, the stability constant of the Cm(III) HSA species is compared to the logK value of Eu(III) HSA. The latter was determined by equilibrium dialysis at pH 7.4 and T = 310 K to be logK = 6.41 ± 0.02 [30]. Although the Eu(III) HSA experiments were performed at different temperature and pH, both stability constants are in good agreement and confirm the similar complexation behaviour of trivalent lanthanides and actinides.

3.3. Complexation studies of Cm(III) with HSA at varying pH and physiological temperature

In addition to the results obtained at room temperature conditions shown above, the complexation of Cm(III) with HSA is investigated at physiological temperature (310 K). Fluorescence spectra are measured in the pH range from 3.5 to 11.5. They correspond to those obtained at room temperature and display the emission bands of the Cm(III) aquo ion at λ_{max} = 593.8 nm, the Cm(III) TRIS/OH^- solvent species at λ_{max} = 598.6 nm, the Cm(III) HSA species at λ_{max} = 603.1 nm and the ternary Cm(III)-OH-HSA species formed in the alkaline pH region.

The species distribution in dependence of the pH is determined by peak deconvolution of the pH dependent emission spectra. Fig. 6 depicts the formation of the Cm(III) HSA species in dependence of pH at room temperature and physiological temperature. In comparison to the results at room temperature, the ratio of the Cm(III) HSA species increases by about 10%. Therefore, the Cm(III) HSA species is the dominating species in a wide range between pH 6.3 and 9.7. Comparison at physiological pH = 7.4 shows an increase of the ratio of the Cm(III) HSA species from about 50% at room temperature to 70% at physiological temperature. Consequently, the complexation of Cm(III) with HSA is an endothermic process which means that the formation of the Cm(III) HSA species plays a more significant role at physiologically relevant conditions (pH 7.4, 310 K, 150 mM NaCl). This is very important with regard to the distribution of incorporated radionuclides, especially trivalent actinides, in the human body.

3.4. Competition titration of Cm(III) HSA with Cu(II) and Zn(II)

The TRLFS experiments give a good description of the complexation of Cm(III) with HSA in dependence of pH, temperature and ligand concentration. However, HSA possesses at least four metal binding sites and the binding site for Cm(III) is not yet explicitly defined. The two

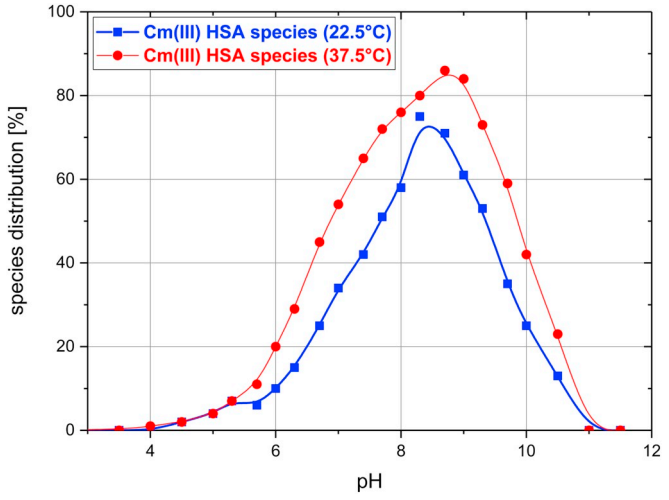

Fig. 6. Formation of the Cm(III) HSA species as a function of pH at room temperature and physiological temperature; c(Cm) = $1.0{\cdot}10^{-7}$ M, c(HSA) = $5.0{\cdot}10^{-6}$ M, TRIS 10 mM, NaCl 150 mM.

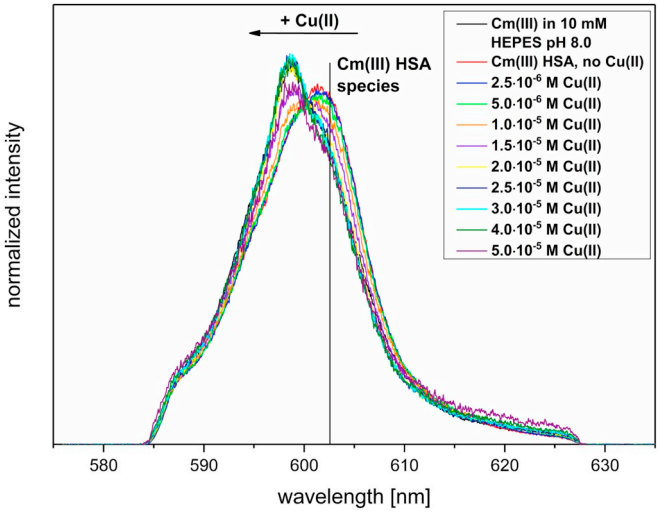

Fig. 7. Normalized fluorescence spectra of Cm(III) with HSA at pH 8.0 in dependence of the Cu(II) concentration; c(Cm) = $1.0{\cdot}10^{-7}$ M, c(HSA) = $5.0{\cdot}10^{-6}$ M, c(Cu) = 0–$5.0{\cdot}10^{-5}$ M, HEPES 10 mM, NaCl 150 mM, T = 296 K.

binding sites with the highest affinities to metal ions are the N-terminal Cu and Ni binding site (ATCUN site or NTS) and the multi metal binding site (MBS), which binds predominantly Cd and Zn.

To identify the HSA binding site for Cm(III) competition titrations with Cu(II) and Zn(II) were performed. Two samples of Cm(III) with HSA at pH 8.0 were prepared and aliquots of a $CuCl_2$ or $ZnCl_2$ stock solution were added stepwise. The emission spectra of the Cu(II) titration are shown in Fig. 7. The spectrum of Cm(III) at pH 8.0 in the absence of HSA and Cu(II) displays an emission maximum at λ_{max} = 598.3 nm and results from the Cm(III) interaction with the solvent. In the presence of HSA the Cm(III) HSA species is formed and the emission band shifts to λ_{max} = 601.6 nm. With increasing Cu(II) concentration the Cm(III) HSA complexation is repressed. The emission band shifts to lower wavelength with increasing Cu(II) concentration until the Cm(III) solvens spectrum is obtained at the end of the titration. These results indicate the complexation of Cm(III) at the predominant Cu(II) binding site, the NTS. This is in good agreement with the fluorescence lifetime of the Cm(III) HSA species displaying four to five water molecules in the inner coordination sphere which are in line with the complexation of Cm(III) at an easily accessible HSA binding site located at the protein surface like the NTS. This is also in good agreement with the results of Montavon et al. on U(VI) HSA interaction indicating complexation of U(VI) at the NTS [32].

Additionally, a competition titration with Zn(II) was performed to verify if Cm(III) complexation also occurs at the MBS (Fig. 8). In contrast to the experiments with Cu(II) a backshift of the emission band of the Cm(III) HSA species to the Cm(III) solvent spectrum is not observed with increasing Zn(II) concentration. Instead, addition of Zn(II) leads to a slight bathochromic shift of the emission band of up to 2 nm. This might be attributed to Zn(II) complexation at a different binding site which is not occupied by Cm(III), most likely at the MBS. The interaction of Zn(II) with amino acid residues of the protein introduces slight changes in the three-dimensional protein structure and influences the coordination environment of the Cm(III) HSA species. The results of the Zn(II) competition titration prove that Cm(III) does not predominantly bind at the preferential Zn(II) binding site, the MBS.

The competition titrations with Cu(II) and Zn(II) are a valuable contribution to the identification of the binding site of Cm(III) with HSA. The results clearly point to a complexation of Cm(III) at the NTS at the N-terminal end of the protein chain. Nevertheless, experiments are required to obtain a detailed understanding of the binding mechanism and structure of the Cm(III) HSA complex.

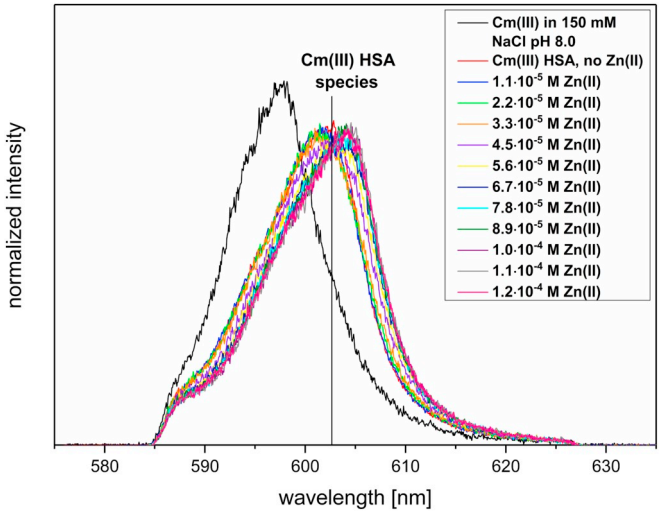

Fig. 8. Normalized fluorescence spectra of Cm(III) with HSA at pH 8.0 in dependence of the Zn(II) concentration; c(Cm) = $1.0 \cdot 10^{-7}$ M, c(HSA) = $5.0 \cdot 10^{-6}$ M, c(Cu) = 0–$1.2 \cdot 10^{-4}$ M, NaCl 150 mM, T = 296 K.

3.5. NMR spectroscopy of Cu(II), Eu(III) and Am(III) HSA

For further confirmation of the NTS being the binding site for trivalent actinides NMR experiments were performed with Cu(II), Eu(III) and Am(III) HSA. As NMR is inherently a rather insensitive method, higher protein and metal ion concentrations, both in the millimolar concentration range, had to be used. For this reason, Am(III), which is available in larger quantities than Cm(III), and Eu(III) as lanthanide analogue for trivalent actinides were used in the NMR experiments.

There are 16 His residues present in HSA. In NMR spectra the His protons appear in the aromatic region, approximately between 6 and 8 ppm. The pH dependency of the His signals was studied by Labro et al. [52]. Bos et al. assigned the signal at 7.5 ppm (pH 8.0) to the His C2 proton of His 3 which is part of the NTS [53]. Addition of Cu(II) to HSA results in a decrease of the peak intensity of this signal (Fig. 9) indicating an interaction between Cu(II) and the His 3 residue upon complexation at the NTS.

The peak intensity of the 7.5 ppm signal assigned to the His 3 C2 proton was also investigated at various Eu(III) and Am(III) concentrations (Fig. 10). In both cases a decrease of the peak intensity with increasing metal ion concentration is observed. This indicates an interaction of Eu(III) and Am(III) with His 3 upon complexation at the NTS, which is in excellent agreement with the results of the competition

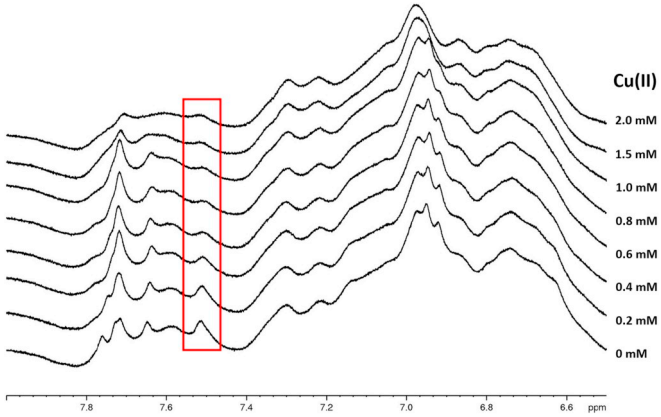

Fig. 9. NMR spectra of Cu(II) HSA at pH 8.0 in dependence of the Cu(II) concentration; c(HSA) = 1 mM, c(Cu(II)) = 0–2 mM, TRIS 10 mM, 10% D_2O, T = 298 K.

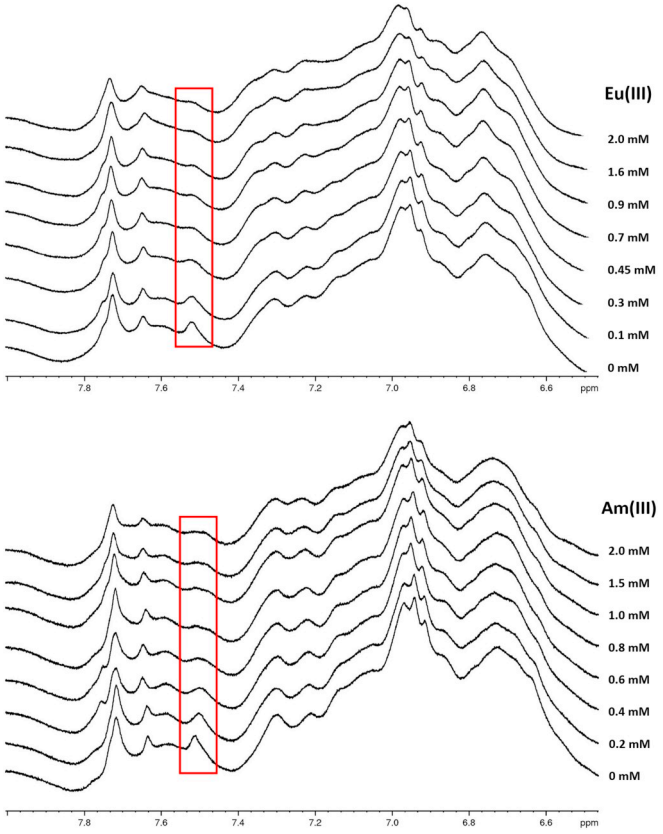

Fig. 10. NMR spectra of Eu(III) HSA (top) and Am(III) HSA (bottom) at pH 8.0 in dependence of the metal ion concentration; c(HSA) = 1 mM, c(Eu(III)) = c(Am(III)) = 0–2 mM, TRIS 10 mM, 10% D_2O, T = 298 K.

titrations of Cm(III) HSA with Cu(II) and Zn(II), also pointing to a complexation of Cm(III) at the NTS.

4. Conclusions

In the present study the Cm(III) HSA interaction was studied. A Cm(III) HSA species was identified and spectroscopically characterized for the first time. The Cm(III) HSA species is dominating the speciation between pH 7.0 and 9.3. The spectroscopic shift of the emission band and the fluorescence lifetime indicate the formation of a Cm(III) complex with the protein with three to four H_2O molecules and five to six coordinating ligands and/or additional anions in the first coordination sphere of Cm(III). For the complex formation at pH 8.0 the conditional stability constant of logK = 6.16 ± 0.50 was determined. Another aim of this work was the identification of the HSA binding site for trivalent actinides and lanthanides. Competition titration experiments with Cu(II) and Zn(II) show that with increasing Cu(II) concentration the Cm(III) HSA complexation is repressed whereas an addition of Zn(II) to Cm(III) HSA has no effect. This points to the complexation of Cm(III) at the NTS which is the primary Cu(II) binding site. These results are supported by NMR experiments with Cu(II), Eu(III) and Am(III) HSA. The peak assigned to the His C2 proton of His 3, which is part of the NTS, decreases with increasing metal ion concentration in all cases. This confirms the complexation of Eu(II) and Am(III) at the Cu(II) binding site NTS.

At physiologically relevant pH (7.4) and temperature (T = 310 K) about 70% of Cm(III) are bound to HSA. Since HSA is the most abundant protein in human blood, Cm(III) complexation to HSA is a possible pathway for the distribution of Cm(III) in particular and trivalent actinides and lanthanides in general in the human body. Therefore, the results presented in this study contribute to a better understanding of

relevant biochemical reactions of incorporated actinides and can be of major importance for the future development of potential decontamination therapies.

References

[1] E. Ansoborlo, L. Bion, D. Doizi, C. Moulin, V. Lourenco, C. Madic, G. Cote, J. Van der Lee, V. Moulin, Radiat. Prot. Dosim. 127 (2007) 97–102.
[2] A.E.V. Gorden, J.D. Xu, K.N. Raymond, P. Durbin, Chem. Rev., vol. 103, 2003, pp. 4207–4282.
[3] E. Ansoborlo, O. Prat, P. Moisy, C. Den Auwer, P. Guilbaud, M. Carriere, B. Gouget, J. Duffield, D. Doizi, T. Vercouter, C. Moulin, V. Moulin, Biochimie 88 (2006) 1605–1618.
[4] D.M. Taylor, J Alloy Compd 271 (1998) 6–10.
[5] Pschyrembel Klinisches Wörterbuch, DeGruyter, 266th Ed. 2014.
[6] S. Sugio, A. Kashima, S. Mochizuki, M. Noda, K. Kobayashi, Protein Eng. 12 (1999) 439–446.
[7] X.M. He, D.C. Carter, Nature 358 (1992) 209–215.
[8] J. Lu, A.J. Stewart, P.J. Sadler, T.J.T. Pinheiro, C.A. Blindauer, Biochem Soc T 36 (2008) 1317–1321.
[9] D.C. Carter, X.M. He, Science 249 (1990) 302–303.
[10] S. Curry, H. Mandelkow, P. Brick, N. Franks, Nat. Struct. Biol. 5 (1998) 827–835.
[11] K.A. Majorek, P.J. Porebski, A. Dayal, M.D. Zimmerman, K. Jablonska, A.J. Stewart, M. Chruszcz, W. Minor, Mol. Immunol. 52 (2012) 174–182.
[12] P.J. Sadler, A. Tucker, J.H. Viles, Eur. J. Biochem. 220 (1994) 193–200.
[13] H. Kozlowski, W. Bal, M. Dyba, T. Kowalik-Jankowska, Coordin Chem Rev 184 (1999) 319–346.
[14] A.J. Stewart, C.A. Blindauer, S. Berezenko, D. Sleep, P.J. Sadler, P Natl Acad Sci USA 100 (2003) 3701–3706.
[15] E.O. Martins, T. Drakenberg, Inorganica Chimica Acta-Bioinorganic Chemistry 67 (1982) 71–74.
[16] P.J. Sadler, J.H. Viles, Inorg. Chem. 35 (1996) 4490–4496.
[17] W. Goumakos, J.P. Laussac, B. Sarkar, Biochem. Cell Biol. 69 (1991) 809–820.
[18] W. Bal, J. Christodoulou, P.J. Sadler, A. Tucker, J. Inorg. Biochem. 70 (1998) 33–39.
[19] W. Bal, M. Sokolowska, E. Kurowska, P. Faller, Bba-Gen Subjects 1830 (2013) 5444–5455.
[20] M. Rozga, M. Sokolowska, A.M. Protas, W. Bal, J. Biol. Inorg. Chem. 12 (2007) 913–918.
[21] M. Sokolowska, K. Pawlas, W. Bal, Bioinorg. Chem. Appl. 2010 (2010).
[22] J. Lu, A.J. Stewart, D. Sleep, P.J. Sadler, T.J.T. Pinheiro, C.A. Blindauer, J. Am. Chem. Soc. 134 (2012) 1454–1457.
[23] E. Ohyoshi, Y. Hamada, K. Nakata, S. Kohata, J. Inorg. Biochem. 75 (1999) 213–218.
[24] M. Sokolowska, M. Wszelaka-Rylik, J. Poznanski, W. Bal, J. Inorg. Biochem. 103 (2009) 1005–1013.
[25] M. Sokolowska, A. Krezel, M. Dyba, Z. Szewczuk, W. Bal, Eur. J. Biochem. 269 (2002) 1323–1331.
[26] I. Correia, T. Jakusch, E. Cobbinna, S. Mehtab, I. Tomaz, N.V. Nagy, A. Rockenbauer, J.C. Pessoa, T. Kiss, Dalton T 41 (2012) 6477–6487.
[27] L. Li, X. Li, X. Qi, G.T. Luo, Spectrosc Spect Anal 24 (2004) 74–77.
[28] Y.J. Jin, W.L. Li, Q.R. Wang, Biochem Bioph Res Co 177 (1991) 474–479.
[29] E. Ohyoshi, S. Kohata, J. Inorg. Biochem. 52 (1993) 157–163.
[30] K. Schomacker, D. Mocker, R. Munze, G.J. Beyer, Appl Radiat Isotopes 39 (1988) 261–264.
[31] M. Ali, A. Kumar, M. Kumar, B.N. Pandey, Biochimie 123 (2016) 117–129.
[32] G. Montavon, C. Apostolidis, F. Bruchertseifer, U. Repinc, A. Morgenstern, J. Inorg. Biochem. 103 (2009) 1609–1616.
[33] J. Michon, S. Frelon, C. Garnier, F. Coppin, J. Fluoresc. 20 (2010) 581–590.
[34] Y. Yang, Y.X. Feng, Y.F. Wang, L. Wang, W.Q. Shi, J Radioanal Nucl Ch 298 (2013) 903–908.
[35] I.J. Kim, R. Klenze, H. Wimmer, European Journal of Solid State and Inorganic Chemistry 28 (1991) 347–356.
[36] N.M. Edelstein, R. Klenze, T. Fanghänel, S. Hubert, Coordin Chem Rev 250 (2006) 948–973.
[37] W.R. Harris, V.L. Pecoraro, Biochemistry 22 (1983) 292–299.
[38] W.R. Harris, B.S. Yang, S. Abdollahi, Y. Hamada, J. Inorg. Biochem. 76 (1999) 231–242.
[39] M.J. Hunter, F.C. Mcduffie, J. Am. Chem. Soc. 81 (1959) 1400–1406.
[40] T. Kimura, G.R. Choppin, J Alloy Compd 213 (/214) (1994) 313–317.
[41] T. Kimura, G.R. Choppin, Y. Kato, Z. Yoshida, Radiochim. Acta 72 (1996) 61–64.
[42] M. Piotto, V. Saudek, V. Sklenář, J. Biomol. NMR 2 (1992) 661–665.
[43] V. Sklenar, M. Piotto, R. Leppik, V. Saudek, J. Magn. Reson. Ser. A 102 (1993) 241–245.
[44] R. Klenze, J.I. Kim, H. Wimmer, Radiochim. Acta 52-3 (1991) 97–103.
[45] J.V. Beitz, J.P. Hessler, Nucl. Technol. 51 (1980) 169–177.
[46] J.V. Beitz, Radiochim. Acta 52-3 (1991) 35–39.
[47] N. Bauer, D.R. Fröhlich, P.J. Panak, Dalton T 43 (2014) 6689–6700.
[48] H. Wimmer, R. Klenze, J.I. Kim, Radiochim. Acta 56 (1992) 79–83.
[49] T. Fanghänel, J.I. Kim, P. Paviet, R. Klenze, W. Hauser, Radiochim. Acta 66 (/67) (1994) 81–87.
[50] N. Bauer, Dissertation, Ruprecht-Karls-Universität Heidelberg, Heidelberg, 2015.
[51] R.D. Shannon, C.T. Prewitt, Acta Crystall B-Stru B 25 (1969) (925-&).
[52] J.F.A. Labro, L.H.M. Janssen, Biochim. Biophys. Acta 873 (1986) 267–278.
[53] O.J.M. Bos, J.F.A. Labro, M.J.E. Fischer, J. Wilting, L.H.M. Janssen, J. Biol. Chem. 264 (1989) 953–959.